For submission to FEBS Letters

Isolation of δ-missulenatoxin-Mb1a, the major vertebrate-active spider δ-toxin from the venom of *Missulena bradleyi* (Actinopodidae)[1]

Simon J. Gunning[a], Youmie Chong[a], Ali A. Khalife[a], Peter G. Hains[b], Kevin W. Broady[c], Graham M. Nicholson[a, *]

Departments of [a]Health Sciences and [c]Cell & Molecular Biology, University of Technology, Sydney, NSW 2007, Australia
[b]Department of Chemistry, University of Wollongong, NSW 2522, Australia

Key words: Spider; Peptide; δ-Missulenatoxin; Sodium channel; Scorpion toxin; δ-Atracotoxin

[1] The protein sequence of δ-missulenatoxin-Mb1a reported in this paper has been submitted to the Swiss Protein database under the SwissProt accession code P83608.

[*] Corresponding author.
Associate Professor Graham M. Nicholson, PhD
Leader, Neurotoxin Research Group
Department of Health Sciences
University of Technology, Sydney
P.O. Box 123
Broadway NSW 2007
Australia

Tel: (61) (2) 9514 2230, Fax: (61) (2) 9514 2228.
E-mail: Graham.Nicholson@uts.edu.au

Abstract The present study describes the isolation and pharmacological characterisation of the neurotoxin δ-missulenatoxin-Mb1a (δ-MSTX-Mb1a) from the venom of the male Australian eastern mouse spider, *Missulena bradleyi.* This toxin was isolated using reverse-phase HPLC and was subsequently shown to cause an increase in resting tension, muscle fasciculation and a decrease in indirect twitch tension in a chick biventer cervicis nerve-muscle bioassay. Interestingly, these effects were neutralised by antivenom raised against the venom of the Sydney funnel-web spider *Atrax robustus*. Subsequent whole-cell patch-clamp electrophysiology on rat dorsal root ganglion neurons revealed that δ-MSTX-Mb1a caused a reduction in peak tetrodotoxin (TTX)-sensitive sodium current, a slowing of sodium current inactivation and a hyperpolarizing shift in the voltage at half-maximal activation. In addition, δ-MSTX-Mb1a failed to affect TTX-resistant sodium currents. Subsequent Edman degradation revealed a 42-residue peptide with unusual N- and C-terminal cysteines and a cysteine triplet (Cys^{14-16}). This toxin was highly homologous to a family of δ-atracotoxins (δ-ACTX) from Australian funnel-web spiders including conservation of all eight cysteine residues. In addition to actions on sodium channel gating and kinetics to δ-ACTX, δ-MSTX-Mb1a caused significant insect toxicity at doses up to 2000 pmol/g. δ-MSTX-Mb1a therefore provides evidence of a highly conserved spider δ-toxin from a phylogenetically distinct spider family that has not undergone significant modification.

Abbreviations: δ-MSTX-Mb1a, δ-missulenatoxin-Mb1a from the Eastern mouse spider *Missulena bradleyi*; TTX, tetrodotoxin; δ-ACTX, δ-atracotoxins from Australian funnel-web spiders; δ-ACTX-Ar1a, δ-atracotoxin-Ar1a (formerly robustoxin) from the Sydney funnel-web spider *Atrax robustus*; δ-ACTX-Hv1a, δ-atracotoxin-Hv1a (formerly versutoxin) from the Blue Mountains funnel-web spider *Hadronyche versuta*; δ-ACTX-Hv1b, δ-atracotoxin-Hv1b from

Hadronyche versuta; δ-ACTX-Hs20.1a, δ-atracotoxin-Hs20.1a from *Hadronyche sp. 20*; Lqh II, anti-mammal α-toxin from the scorpion *Leiurus quinquestriatus hebraeus*; Aah-II, anti-mammal α-toxin from the scorpion *Androctonus australis hector*; LqhαIT, α-insect toxin from the scorpion *Leiurus quinquestriatus hebraeus*; SDS-PAGE, sodium dodecyl sulphate-polyacrylamide gel electrophoresis; PVDF, polyvinylidene fluoride; BSA, bovine serum albumin; PBS, phosphate-buffered saline; TBS, tris-buffered saline; FWS-AV, Sydney funnel-web spider antivenom; rp-HPLC, reverse-phase high performance liquid chromatography; TFA, trifluoroacetic acid; BCA, bicinchoninic acid; DRG, dorsal root ganglion; HEPES, N-2-hydroxyethylpiperazine-N-2-ethanesulfonic acid; TEA, tetraethylammonium; MALDI-TOF, matrix-assisted laser desorption/ionisation – time-of-flight; PTH, phenylthiohydantoin; (+)-TC, (+)-tubocurarine; LD_{50}, median lethal dose; PD_{50}, median paralytic dose; ApB, anthopleurin-B from the sea anemone *Anthopleura xanthogrammica*; Magi 4 from the spider *Macrothele gigas*.

1. Introduction

Australian mouse spiders (Araneae: Mygalomorphae: Actinopodidae) are one of the oldest groups of spiders in the Australo-Papuan region. Importantly, the male Eastern mouse spider (*Missulena bradleyi*), restricted to the East coast of mainland Australia, can cause systemic envenomation in humans. The symptoms of envenomation, including muscle fasciculation, tachycardia, dyspnoea, and profuse sweating, are remarkably similar to those reported for Australian funnel-web spiders (Aranaea: Mygalomorphae: Hexathelidae: Atracinae). The only reported case of severe envenomation involved a 19-month-old girl who lost consciousness within 30 minutes of being bitten on the finger by a male *M. bradleyi*. The administration of Sydney funnel-web spider antivenom, raised against *Atrax robustus* venom, surprisingly produced a dramatic improvement in her condition and a full recovery was made following a second dose of antivenom [1]. This prompted a recent study to characterise the pharmacological actions of mouse spider venom. Whole male *M. bradleyi* venom caused rapid muscle fasciculation, a large contracture and a rapid decrease in indirectly-evoked twitches in the chick biventer cervicis muscle, with activity blocked by *A. robustus* antivenom [2]. These actions were found to be due to a reduction in the rate of tetrodotoxin (TTX)-sensitive sodium current inactivation and a hyperpolarizing shift in the threshold of activation of TTX-sensitive sodium currents [2]. The modulation of sodium channel gating and kinetics, and reversal by *A. robustus* antivenom, indicate that the venom from male *M. bradleyi* may contain vertebrate-active neurotoxins that have a similar action to those found in Australian funnel-web spider venoms, despite the fact that mouse spiders are taxonomically distinct from funnel-web spiders.

Previous studies on the venom of Australian funnel-web spiders have revealed a number of toxins, called atracotoxins (ACTX), that are responsible for the neurotoxic action seen with

whole venom (for a review see [3]). However, the lethal toxins responsible for the major primate-specific symptoms of envenomation are the δ-ACTX shown to target the voltage-gated sodium channel (for a review see [4]). To date, four δ-ACTX have been identified, these include δ-ACTX-Ar1a from the Sydney funnel-web spider (*Atrax robustus)* [5], δ-ACTX-Hv1a [6] and –Hv1b [7] from the Blue Mountains funnel-web spider (*Hadronyche versuta*) and δ-ACTX-Hs20.1a from *Hadronyche* sp. 20 [4]. All δ-ACTX are highly homologous 42-residue peptides with a high proportion of basic residues and are cross-linked by four conserved intramolecular disulfide bonds. These peptide, like many spider neurotoxins, also contain an 'inhibitor cystine-knot' (ICK) motif [8-10]. δ-ACTX produce a slowing of TTX-sensitive sodium current inactivation, a modest hyperpolarizing shift in the voltage-dependence of activation and a reduction in peak sodium current [4,7,11,12]. This results in spontaneous repetitive firing accompanied by plateau potentials [13,14]. Of great interest has been the finding that δ-ACTX, in addition to being mammalian toxic, are also insecticidal. Both δ-ACTX-Ar1a and –Hv1a are toxic by lateroventral injection into crickets [15] and target the insect voltage-gated sodium channel to cause similar actions on neuronal excitability as seen in vertebrate preparations [13]. Notably, these actions on insect and mammalian voltage-gated sodium channels are similar, but not identical, to the mechanism of action of scorpion α-toxins and sea anemone toxins [16,17].

Neurochemical studies have shown that at nanomolar concentrations δ-ACTX compete with both anti-mammalian (eg. Lqh-II and Aah-II) and anti-insect (eg LqhαIT) scorpion α-toxins for neurotoxin receptor site-3 on voltage-gated sodium channels [15,18,19] (for a review of sodium channel neurotoxin receptor sites see Gordon [20]). Therefore, it is clear that the δ-ACTXs are extremely potent and define a new class of toxins affecting both insect and mammalian voltage-gated sodium channels.

Interestingly, the three-dimensional fold of δ-ACTX is different from the previously determined structures of all other site-3 neurotoxins despite similar actions on sodium current inactivation [8]. At present, the toxin pharmacophore of δ-ACTX is unknown but is believed to involve a number of basic residues distributed in a topologically similar manner to basic residues in scorpion α-toxins and sea anemone toxins despite distinctly different protein scaffolds [8]. This is supported by the finding that δ-ACTX-Hv1b, a neurotoxin that is devoid of insecticidal activity and has reduced mammalian activity, lacks several N-terminal basic residues [7].

The present investigation describes the biochemical and pharmacological characterisation of a novel neurotoxin, δ-MSTX-Mb1a, from the phylogenetically distinct spider family Actinopodidae. This spider neurotoxin has a similar mode of action and primary structure to the δ-ACTX and provides further evidence for the key role of N-terminal basic residues in the action of δ-ACTX.

2. Materials and methods

2.1. Venom electrophoresis and Western blotting

Crude venom from male and female Eastern mouse spiders (*M. bradleyi*) was collected as previously described [2]. Sodium dodecyl sulphate-polyacrylamide gel electrophoresis (SDS-PAGE) of *M. bradleyi* venom was performed under reducing conditions according to the method of Laemmli [21] using 10-20% Tris-tricine gradient gels (Novex, San Diego, CA, USA). The molecular weight marker lane consisted of markers of 3.4 to 26.6 kDa (Life Science Research products Regents Park, NSW). Following electrophoresis, protein bands were stained using silver nitrate.

Western blotting was performed following initial SDS-PAGE electrophoresis as described above. Proteins were transblotted onto PVDF membrane (Biorad Laboratories, Hercules, CA, USA) in Tris-tricine-methanol transfer buffer using 200 mA constant current for 1 hour. The PVDF membrane was incubated with 3% w/v bovine serum albumin (BSA) in phosphate-buffered saline (PBS) for 1 hour at room temperature. It was then washed in tris-buffered saline (pH 8.0)-Tween 0.05% v/v (TBS-Tween), followed by incubation with funnel-web spider antivenom raised against male Sydney funnel-web spider (*Atrax robustus*) venom (FWS-AV) (Commonwealth Serum Laboratories, Melbourne) at a dilution of 1:500 for 1 hour. The washing step was repeated and the blot was then incubated with a 1:5000 dilution of the secondary antibody, alkaline phosphatase conjugated goat-anti-rabbit IgG (Sigma Laboratories, St Louis, MO, USA), for 1 hour. It was then washed again with TBS-Tween and developed with 5-bromo-4-chloro-indoyl phosphate *p*-toluidine plus nitro-blue tetrazolium.

2.2. Toxin purification and sequencing

Pooled venom was initially fractionated using reverse-phase (rp)-HPLC employing a Vydac analytical column (C_{18}, 4.6 × 250 mm, 5 μm) on a Shimadzu HPLC system. Peptide peaks were monitored at an absorbance of 215 nm. Elution of venom peptide components was achieved using a linear gradient of 5-60% v/v acetonitrile/0.1% v/v trifluoroacetic acid (TFA) over 55 min at a flow rate of 1 ml/min. Selected fractions were subjected to vertebrate toxicity bioassays using a chick biventer cervicis nerve-muscle preparation to determine vertebrate toxicity (see section 2.3). The major toxic fraction, δ-MSTX-Mb1a (peak a in Figure 1C), eluted around 33% acetonitrile concentration and was further purified on an analytical C_{18} rp-HPLC column using a linear gradient of 5-32% acetonitrile/0.1% TFA over 5 min, then 32-34% acetonitrile/0.1% TFA

over 20 min, at a flow rate of 1 ml/min. Purified toxin was collected, lyophilised and stored at –20 ˚C until required. Toxin quantification was performed using a BCA (bicinchoninic acid) Protein Assay Kit (Pierce, Rockford, IL, USA) using BSA as a standard. Absorbances were read at 560 nm on a Titertek Multiscan microplate reader (Eflab, Finland). The molecular mass was determined by electrospray ionisation mass spectrometry. In preparation for amino acid sequencing, the toxin was reduced and cysteine residues were pyridylethylated as described previously [8]. The reduced, pyridylethylated toxin was purified using rp-HPLC as described previously [8], then the entire peptide sequence was obtained from a single sequencing run on an Applied Biosystems/Perkin Elmer Procise 492 cLC protein sequencer.

2.3. Chick isolated biventer cervicis nerve-muscle bioassay

Vertebrate toxicity was confirmed by the use of an isolated chick biventer cervicis nerve-muscle preparation as described previously [22,23]. Briefly, biventer cervicis muscles with attached nerve were removed from male Australorp chicks (1-4 days-old), mounted in 8-ml organ baths and bathed in Krebs-Henseleit solution containing (in mM): NaCl 118.4, KCl 4.7, $CaCl_2$ 2.5, $MgSO_4$ 1.2, KH_2PO_4 1.2, $NaHCO_3$ 25.0, D-glucose 11.1, pH 7.4. The muscle was maintained at 34 °C and constantly carbogenated with 95% O_2 and 5% CO_2. Twitch contractions were elicited by indirect supramaximal stimulation of the motor nerve (supramaximal voltage, 0.05 ms, 0.1 Hz) via ring electrodes connected to a Grass S88 stimulator. Isometric contractions of the muscle were recorded using a Neomedix isometric force transducer, connected to a T-218 amplifier and a MacLab/4s data acquisition system (AD Instruments, Castle Hill, NSW, Australia) connected to a Centris 650 Macintosh computer. In the absence of electrical stimulation, responses to exogenous acetylcholine (1 mM, 30 s) and KCl (40 mM, 30 s) were

obtained prior to the addition of venom and at the conclusion of the experiment. Preparations were allowed to equilibrate for at least 30 minutes with continuous stimulation before the addition of venom or antivenom. All animal experimentation was approved by the joint Animal Care and Ethics Committee of the University of Technology, Sydney and the Royal North Shore Hospital, Sydney, Australia.

2.4. Electrophysiological studies

Acutely dissociated dorsal root ganglion (DRG) neurons were prepared from 4-12 day-old Wistar rats and maintained in short-term primary culture using the method described by Nicholson et al. [11]. Voltage-clamp recordings were made with the whole-cell patch-clamp technique [24] using an AxoPatch 200A patch-clamp amplifier (Axon Instruments, Foster City, CA, USA). Micropipettes were pulled from borosilicate glass capillary tubing (Corning 7052 Glass, Warner Instruments) and had d.c resistances of 0.8–2.0 MΩ.

To record macroscopic sodium currents, micropipettes were filled with a solution of the following composition (in mM): CsF 135; NaCl 10; N-2-hydroxyethylpiperazine-N-2-ethanesulfonic acid (HEPES) 5; with the pH adjusted to 7.0 with 1 M CsOH. The external bathing solution contained (in mM): NaCl 30; $MgCl_2$ 1; $CaCl_2$ 1.8; CsCl 5; KCl 5; D-glucose 25; HEPES 5; tetraethylammonium (TEA)-Cl 20; tetramethylammonium chloride 70; with the pH adjusted to 7.4 with 1 M TEA-OH.

The osmolarity of both solutions was adjusted to 290–300 mOsm/L with sucrose to reduce osmotic stress. The external solution was applied to the perfusion chamber via a gravity-fed perfusion system and the flow rate maintained at 0.5 ml/min using a Gilmont flowmeter (Barrington, IL, USA). Data were recorded at room temperature (20–23 °C) which did

not fluctuate more than 1 °C during the course of an experiment. In all voltage-clamp experiments the holding potential was –80 mV and the sodium concentration of the external solution was reduced to 30 mM to improve series resistance compensation and to avoid saturation in the recording system [25]. Inverted voltage-clamp command pulses were applied to the bath through a Ag/AgCl pellet/3 M KCl-agar bridge. The liquid junction potential between internal and external solutions was approximately –6 mV, and all data were compensated for this value.

Large round DRG cells with diameters of 30-50 μm were selected for experiments. Larger cells from older animals tended to express fast TTX-sensitive sodium currents (I_{Na}) whilst smaller cells tended to express predominately TTX-resistant I_{Na} [26]. In those experiments that assessed the actions of the toxin on TTX-resistant I_{Na}, 200nM TTX was applied to the external solution to eliminate any residual TTX-sensitive I_{Na}. Only those cells that exhibited less than 10% TTX-resistant I_{Na}, as determined from differences in the steady-state sodium channel inactivation profile, were used to determine the actions of toxin on TTX-sensitive I_{Na}. After breaking through the membrane, experiments did not commence for a period of 15-20 min to allow for the complete block of calcium and potassium currents and any fast time-dependent shifts in steady-state inactivation. The experiments used in this study were rejected if there were large leak currents or currents showed signs of poor space clamping such as an abrupt activation of currents upon relatively small depolarising pulses.

Stimulation and recording were both controlled by an AxoData® data acquisition system (Axon Instruments) running on an Apple Macintosh Quadra 700. Data was filtered at 5 kHz (4 pole low-pass Bessel filter) and digital sampling rates were between 15 and 25 kHz depending on voltage protocol length. Leakage and capacitive currents were digitally subtracted with P-P/4 procedures [27] and series resistance compensation was set at >80% for all cells. Data analysis

was performed off-line following completion of the experiment. Mathematical curve fitting employed algorithms available in KaleidaGraph® for Macintosh using a non-linear least squares method. The curve fits for the *I*/*V* data were obtained using the following equation:

$$I_{Na} = g_{max}\left(1 - \left(\frac{1}{1+\exp\left[\left(V - V_{1/2}\right)/s\right]}\right)\right)\left(V - V_{rev}\right) \qquad (1)$$

where I_{Na} is the amplitude of the peak sodium current at a given potential, V, g_{max} is the maximal sodium conductance, $V_{1/2}$ is the voltage at half-maximal activation, s is the slope factor and V_{rev} is the reversal potential.

2.5. Invertebrate toxicity assays

Insect toxicity was determined by latero-ventral thoracic injection of the purified toxin into 3rd-4th instar House crickets nymphs (*Acheta domesticus*, sex undetermined) as described previously [28] at doses up to 2,000 pmol/g. Crickets received injections of toxin dissolved in insect saline of the following composition (in mM): NaCl 200, KCl 3.1, $CaCl_2$ 5, $MgCl_2$ 4, HEPES 10, sucrose 50, pH 7.4. Insects were monitored for 72 hours post-injection for signs of paralysis or lethality.

2.6. Statistics

Comparisons of two sample means were made using a Wilcoxon signed-rank test or paired Student's *t*-test (as specified). A test was considered to be significant when $P<0.05$. Data, when quantified, was expressed as mean ± standard error of the mean (SEM).

3. Results

3.1. Venom electrophoresis and Western blotting

SDS-PAGE revealed considerable variability in the number of protein bands between pooled male and female *M. bradleyi* venom. In particular, constant bands were only present around 7 kDa and 90 Da. In addition, separation patterns of both male and female venom was less complex than funnel-web spider venoms [29]. Notably, male venom appears to have a band around 4900 Da that is absent from female venom (see band marked with * in Fig. 1A). It has been previously reported that female *M. bradleyi* venom does not produce neurotoxicity in vertebrate nerve-muscle preparations [2] and that male venom appears to contain a vertebrate-active neurotoxin with similar actions as δ-ACTX that have a molecular weight of ~4900 Da.

Given that Sydney funnel-web spider antivenom (FWS-AV) reverses the effects of male *M. bradleyi* envenomation, we assessed if FWS-AV would bind to protein fractions in either male or female venom. Western blotting revealed that FWS-AV bound to protein fractions above a molecular weight of 14 kDa. There was little antivenom binding to protein fractions between 5 and 14 kDa. importantly, only male venom showed bands less than 5 kDa consistent with the presence of a possible δ-ACTX-like neurotoxin (see band marked with * in Fig. 1B).

3.2. Toxin Purification

A vertebrate-active neurotoxin in male *M. bradleyi* venom was purified by rp-HPLC. Figure 1C shows a rp-HPLC chromatogram of pooled venom. The fraction containing the toxin eluted at 33% acetonitrile/0.1% TFA (Peak *a*, Fig. 1C). This peak was found to cause strong muscle contracture, fasciculation and to decrease nerve-evoked twitch contractions of chick isolated biventer cervicis muscle (data not shown) similar to those elicited by δ-ACTX-Hv1a and other

Australian funnel-web spider venoms [29]. This fraction was pooled and lyophilised, and further purification, using C_{18} rp-HPLC with a shallow acetonitrile gradient, yielded three distinct components (Fig. 1D). The major peak, labelled peak *b* in Figure 1D, was subsequently shown to be the most active component in the chick biventer cervicis nerve-muscle assay. MALDI-TOF mass spectrometry revealed that the molecular mass of the peptide peak *b* was 4933 ± 1 Da.

3.3. Determination of amino acid sequence

Peak *b* was reduced and the cysteines pyridylethylated in preparation for N-terminal amino acid sequencing to assist in determining the number of cysteine residues. In addition, phenylthiohydantoin(PTH)-Cys with a pyridylethylated sidechain is stable during automated N-terminal amino acid sequencing and therefore allows positive identification of Cys residues.

Mass spectral analysis of the pyridylethylated toxin indicated that it contained eight cysteine residues. The amino acid sequence of the toxin (see Figure 2), obtained in a single sequencing run without the need to resort to proteolytic digestion, revealed that it contains 42 residues, including eight cysteines. Importantly, it possesses both N- and C-terminal cysteines and an unusual cysteine triplet ($Cys^{14\text{-}16}$). The predicted mass of 4934 Da for the fully oxidised peptide, in which the eight cysteine residues form four disulphide bonds, is consistent with the mass spectral analysis.

The toxin displayed significant homology with three other Australian funnel-web spider toxins, δ-ACTX-Hv1a [2] and δ-ACTX-Hv1b [7] isolated from the venom of the female Blue Mountains funnel-web spider, *Hadronyche versuta*, and δ-ACTX-Ar1a [21] isolated from the venom of the male Sydney funnel-web spider, *A. robustus*. The sequence shows conservation in the number and spacing of cysteine residues. When conservative substitutions are taken into

consideration, the homology with other δ-ACTX ranges from 76 to 98%. The toxin has nine amino acid substitutions relative to δ-ACTX-Hv1a, its closest ortholog (see Fig. 2). In addition, the toxin shows 67% sequence homology to the recently identified sodium channel toxin Magi 4 from the hexathelid spider *Macrothele gigas* [30].

Based on the sequence homology and functional similarities (see below) with δ-ACTX, we have named the toxin δ-missulenatoxin-Mb1a (δ-MSTX-Mb1a) in accordance with the nomenclature previously described for toxins isolated from Australian funnel-web spiders [5]. The sequence of δ-MSTX-Mb1a has been deposited in the SWISS-PROT Databank under the accession number P83608.

Although the pairing of cysteines was not determined experimentally, the high homology in primary structure with previously described spider δ-toxins strongly suggests that δ-MSTX-Mb1a conforms to an inhibitor cystine-knot motif (Cys1-Cys4, Cys2-Cys6, Cys3-Cys7, Cys5-Cys8)[10,31] as has been observed for most spider neurotoxins.

3.4. Effects of δ-MSTX-Mb1a on the isolated chick biventer cervicis nerve-muscle preparation

In the indirectly-stimulated chick biventer cervicis muscle, δ-MSTX-Mb1a (85 nM) caused a rapid muscle contracture (increase in resting tension), associated with muscle fasciculation and a decrease in twitch tension (Fig. 3A). However, δ-MSTX-Mb1a had no significant effect on responses to acetylcholine (1 mM: 2.4 ± 1.4 g before toxin, 2.38 ± 1.4 g after toxin), carbachol (20 μM: 1.52 ± 0.8 g before toxin, 1.45 ± 0.8 g after toxin) or KCl (40 mM 2.78 ± 1.6 g before toxin, 2.23 ± 1.3 g after toxin) (n = 3, P >0.05, Wilcoxon signed-rank test) (data not shown). The contracture induced by δ-MSTX-Mb1a (85 nM) was completely abolished by the skeletal muscle

nicotinic receptor antagonist (+)-tubocurarine (10 μM) and by the sodium channel blocker TTX (200 nM) (Fig. 3B, C).

A 10-minute pre-treatment of the indirectly stimulated chick biventer cervicis muscle with 0.6 U/ml Sydney funnel-web spider antivenom completely prevented the contracture, fasciculations and the attenuation of twitches caused by δ-MSTX-Mb1a (85 nM) (n = 3, Fig. 4A). It was also found that the effects of δ-MSTX-Mb1a on the nerve-muscle preparation could be reversed by subsequent addition of Sydney funnel-web spider antivenom (0.6 U/ml) (n = 3, Fig. 4B).

3.5. Effects of δ-MSTX-Mb1a on voltage-gated sodium currents

Under voltage-clamp conditions, δ-ACTXs have been previously shown to cause a concentration-dependent reduction in peak TTX-sensitive I_{Na} amplitude and slowing of I_{Na} inactivation [4,7,11,12]. Figure 5A shows the effect of δ-MSTX-Mb1a on TTX-sensitive I_{Na}. At 30 nM, δ-MSTX-Mb1a reduced peak TTX-sensitive I_{Na} amplitude by 24 ± 8% (n = 3, $P < 0.05$, paired Student's t-test) and slowed the rate of TTX-sensitive I_{Na} inactivation. Analysis of the toxin effect on inactivation was estimated by measuring the I_{Na} remaining after 50 ms following a step depolarization to indicate the proportion of channels with permanently modified inactivation. At –10 mV the remaining current was 19.2 ± 4.2% (n = 3) of control peak I_{Na}. Since the reduction in peak I_{Na} at 30 nM was found to be similar for both δ-MSTX-Mb1a and both δ-ACTX-Hv1a and –Ar1a [11], we conclude that δ-MSTX-Mb1a is approximately equipotent with δ-ACTX-Hv1a and –Ar1a on TTX-sensitive sodium channels. Similar to δ-ACTX, the reduction in sodium current amplitude and slowing of current inactivation produced by δ-MSTX-Mb1a was only partially reversible after prolonged washing with toxin-free solution. In

marked contrast to its action on TTX-sensitive sodium channels, δ-MSTX-Mb1a (300 nM), like other δ-ACTX [11,12], failed to significantly alter either the amplitude or time course of TTX-resistant I_{Na} (Fig. 5E).

Previous studies have shown that δ-ACTX shift the threshold of activation of TTX-sensitive I_{Na} in the hyperpolarizing direction [4,7,11,12]. Analysis of the *I*/*V* relationship of TTX-sensitive I_{Na} in the presence of 30 nM δ-MSTX-Mb1a (Fig 5B-D) revealed a similar 10 mV hyperpolarizing shift in the threshold of sodium channel activation. Data were normalised and fitted using a single Boltzmann distribution. δ-MSTX-Mb1a caused a hyperpolarizing shift in the voltage at half maximal activation ($V_{1/2}$) from –22.6 ± 1.4 mV (n = 3, $P < 0.05$, paired Student's *t*-test) in controls to –33.2 ± 0.4 mV with no change in the slope factor *s*. Figure 5 also shows that these changes occurred in the absence of significant changes in the reversal potential which were only slightly decreased from 29.8 mV (calculated from Nernst equation) by 1.2 ± 0.5 mV ($P >$ 0.05 paired Student's *t*-test). These changes could not be explained by spontaneous time-dependent shifts in the voltage dependence of activation, which in general are <5 mV in DRG neurons (G. Nicholson, unpublished results).

Consistent with δ-ACTXs, and in marked contrast to its action on TTX-sensitive I_{Na}, δ-MSTX-Mb1a (300 nM) failed to significantly alter the voltage-dependence of activation of TTX-resistant I_{Na} (see Fig. 5F-H).

3.6. Insecticidal activity of δ-MSTX-Mb1a

δ-ACTX-Hv1a was previously shown to be a moderately potent insecticidal toxin, with an LD_{50} of 770 pmol/g in house crickets (*A. domesticus*) [15] Furthermore, δ-ACTX-Hv1a caused contractile paralysis at significantly lower doses (PD_{50} = 200 pmol/g), with the higher LD_{50}

reflecting the fact that most crickets recover from the contractile paralysis at doses near or below the PD_{50} [15]. However δ-ACTX-Hv1b showed a complete absence of insect toxicity at doses up to 2,000 pmol/g. Crickets were injected with δ-MSTX-Mb1a at doses up to 2,000 pmol/g and within 20 minutes of injection showed signs of neurotoxicity including continuous and involuntary spasms of the appendages, abdomen and head. There was a moderate loss of co-ordination when walking, and some crickets showed marked latero-flexion of their abdomen. Interestingly, there was some reversal of these signs of toxicity, with the exception of abdominal latero-flexion, within 24 hours post-injection and at doses below 1,000 pmol/g insects recovered completely. Nevertheless, lethality was observed in 60% of crickets at a dose of 2,000 pmol/g after 48 hours indicating that δ-MSTX-Mb1a is approximately 2-fold less toxic to crickets than δ-ACTX-Hv1a.

4. Discussion

This paper describes the isolation and characterisation of a peptide neurotoxin that modulates vertebrate sodium channel inactivation from a spider species unrelated to Australian funnel-web spiders (Hexathelidae). N-terminal sequencing showed that the actinopodid toxin δ-MSTX-Mb1a corresponds to a 42-residue peptide of molecular weight 4,933 Da that is clearly a close ortholog of δ-ACTX-Hv1a and related hexathelid spider δ-toxins. The cysteine spacing with characteristic N- and C-terminal cysteines and cysteine triplet, characteristic of spider δ-toxins, strongly suggests that this novel toxin belongs to the inhibitor cystine-knot motif group of peptides. δ-MSTX-Mb1a mimics the neurotoxicity of δ-ACTX-Hv1a [29], causing a sustained contracture and muscle fasciculation of vertebrate skeletal muscle, consistent with similar signs of envenomation in-vivo. This appears to be the result of spontaneous neurotransmitter release from motor nerve terminals and not an alteration in postjunctional excitation-contraction coupling. This was evident from the fact that responses of slow muscle fibres to KCl and acetylcholine in the chick nerve-muscle preparation were unaffected and the contracture was blocked by prior application of TTX or (+)-tubocurarine. These presynaptic actions to induce neurotransmitter release, particularly in cholinergic nerve fibres, are consistent with those reported in clinical cases of severe envenomation or *in-vitro* studies with whole venom [1,2]. In addition, the actions of the toxin could be neutralised or reversed by Sydney funnel-web spider antivenom consistent with previous *in-vitro* and *in-vivo* studies [2]. The present findings provide additional evidence for the cross-reactivity of Sydney funnel-web spider antivenom and supports the potential effectiveness of this antivenom in cases of systemic envenomation by male *M. bradleyi*.

Given that previously characterised spider δ-toxins are, by definition, potent modulators of sodium channel inactivation [14,15], we investigated whether δ-MSTX-Mb1a modulated sodium channel gating or kinetics. The findings of this study demonstrate that δ-MSTX-Mb1a has selective effects on TTX-sensitive I_{Na} including: (*a*) a slowing of channel inactivation; (*b*) a reduction in peak current amplitude; and (*c*) shifts in the voltage-dependence of activation. In contrast, and consistent with spider δ-toxins, TTX-resistant sodium channel gating and kinetics remained unaffected.

These actions, especially the slowing of I_{Na} inactivation in the absence of large shifts in the voltage-dependence of activation or profound slowing of deactivation, indicates that δ-MSTX-Mb1a acts in a manner similar to scorpion α-toxins, sea anemone toxins, and previously characterised δ-ACTX that bind to neurotoxin receptor site-3. The above actions of δ-MSTX-Mb1a indicate that it inhibits conversion of the voltage-gated sodium channel from the open to the inactivated state, resulting in sodium currents remaining at membrane potentials where inactivation is normally complete. This is qualitatively similar to all other δ-ACTX, apart from the vertebrate-selective δ-ACTX-Hv1b that appears to be approximately 15- to 30-fold less potent in its modulation of vertebrate sodium channel gating and kinetics. In addition, δ-MSTX-Mb1a like other spider δ-toxins, except δ-ACTX-Hv1b, possesses both insect and vertebrate toxicity, albeit with slightly reduced insecticidal potency. This is presumably due to binding to insect voltage-gated sodium channels at site-3 to slow inactivation as has been previously observed with δ-ACTX-Hv1a [13,15,32].

Given the high similarity in primary sequence, cysteine spacing and bioactivity, as well as a common antibody epitope, it seems plausible that δ-MSTX-Mb1a shares a similar inhibitor cystine-knot motif, 3D-structure and importantly a similar pharmacophore to that of δ-ACTX.

Unfortunately, work to identify the bioactive surface of δ-ACTX has been hampered by the four disulfide bonds preventing the refolding of synthetic or recombinant toxin in sufficient yields to attempt mutagenesis studies. Nevertheless, critical residues involved in δ-ACTX binding have been delineated by matching topologically related residues on the bioactive surface of LqhαIT, a scorpion α-toxin. Previous mutagenesis studies have shown that several basic, nonpolar and aromatic residues that constitute the bioactive surface of LqhαIT [33] cluster in a similar fashion on the counterpart surface of the site-3 toxins Aah-II and ApB and, interestingly, also appear on the surface of both δ-ACTX-Hv1a and –Ar1a, despite distinctly different protein scaffolds [32]. In the spider δ-toxins, that are toxic to both insects and vertebrates, these are the positively charged residues Lys^3, Lys^4, Arg^5 and Lys^{10} , the nonpolar Asn^6 and the aromatic residues Trp^7 and Tyr^{22}/ Tyr^{25} [32] (for a review see [4]). Importantly these residues are conserved in the ortholog δ-MSTX-Mb1a lending further support to the hypothesis that they form the bioactive surface of spider δ-toxins targeting site-3 of the sodium channel.

Importantly, close inspection of the primary structure of the spider δ-toxins reveals that a number of amino acids are not conserved between δ-ACTX-Hv1b and other hexathelid spider δ-like toxins including Magi 4 from *Macrothele gigas* [30] and the actinopodid spider δ-toxin, δ-MSTX-Mb1a (see Fig. 2). It is assumed that Magi 4 is a spider δ-toxin since it shows sequence homology to δ-ACTX, is lethal to mammals and insects, and competes with LqhαIT for site-3 on insect sodium channels. Interestingly though, it fails to compete with Lqh-II for binding to rat brain synaptosomes and therefore shows unusual binding characteristics despite being toxic when injected intracerebroventricularly in mice [30]. Significantly, δ-ACTX-Hv1b lacks insect toxicity and has a 15- to 30-fold reduction in vertebrate toxicity, however, it has non-conservative K4S, R5D, and Y22K substitutions in comparison to spider δ-toxins and Magi 4 that are all known to

be toxic to insects and vertebrates. This lends support to the hypothesis that these basic and aromatic residues are important for full vertebrate and insect activity.

The similar disposition of these residues on the distinctly dissimilar 3D surface of site-3 peptide toxins from scorpions, sea anemones and spiders, demonstrates the putative route of convergent evolution of receptor site-3 ligands. In addition, the highly conserved sequence homology between two phylogenetically distinct and primitive spider families (Actinopodidae vs. Hexathelidae) provides evidence to suggest that there is strong selection pressure to maintain such highly toxic peptides despite potential evolutionary mutation. This provides strong evidence of the highly optimised nature of peptide neurotoxins especially those from spider venoms.

Acknowledgments: This work was supported in part by an Australian Research Council research grant to G.M.N. and K.W.B. The authors would like to thank Ms Michelle Little for assistance with the maintenance and milking of the mouse spider colony. We are also grateful to the Ms Mary Raynor and staff at the Australian Reptile Park for assistance on the collection of the spiders.

References

[1] Underhill, D. (1987) in: Australia's Dangerous Creatures, pp. 175 (Sutherland, S.K., Ed.) Readers Digest Services, Sydney.

[2] Rash, L.D., Birinyi-Strachan, L.C., Nicholson, G.M. and Hodgson, W.C. (2000) Br. J. Pharmacol. 130, 1817-1824.

[3] King, G.F., Tedford, H.W. and Maggio, F. (2002) J. Toxicol.-Toxin Rev. 21, 359-389.

[4] Nicholson, G.M., Little, M. and Birinyi-Strachan, L.C. (2003) Toxicon in press.

[5] Sheumack, D.D., Claassens, R., Whiteley, N.M. and Howden, M.E.H. (1985) FEBS Lett. 181, 154-156.

[6] Brown, M.R., Sheumack, D.D., Tyler, M.I. and Howden, M.E.H. (1988) Biochem. J. 250, 401-405.

[7] Szeto, T.H., Birinyi-Strachan, L.C., Wang, X.-H., Smith, R., Connor, M., Christie, M.J., King, G.F. and Nicholson, G.M. (2000) FEBS Lett. 470, 293-299.

[8] Fletcher, J.I., Chapman, B.E., Mackay, J.P., Howden, M.E.H. and King, G.F. (1997) Structure 5, 1525-1535.

[9] Pallaghy, P.K., Alewood, D., Alewood, P.F. and Norton, R.S. (1997) FEBS Lett. 419, 191-196.

[10] Pallaghy, P.K., Neilsen, K.J., Craik, D.J. and Norton, R.S. (1994) Protein Sci. 3, 1833-1839.

[11] Nicholson, G.M., Willow, M., Howden, M.E.H. and Narahashi, T. (1994) Pflügers Archiv. (Eur. J. Physiol.) 428, 400-409.

[12] Nicholson, G.M., Walsh, R., Little, M.J. and Tyler, M.I. (1998) Pflügers Archiv. (Eur. J. Physiol.) 436, 117-126.

[13] Grolleau, F., Stankiewicz, M., Birinyi-Strachan, L.C., Wang, X.-H., Nicholson, G.M., Pelhate, M. and Lapied, B. (2001) J. Exp. Biol. 204, 711-721.

[14] Alewood, D., Birinyi-Strachan, L.C., Pallaghy, P., Norton, R., Nicholson, G.M. and Alewood, P.F. (2003) Biochemistry in press.

[15] Little, M.J., Wilson, H., Zappia, C., Cestèle, S., Tyler, M.I., Martin-Eauclaire, M.-F., Gordon, D. and Nicholson, G.M. (1998) FEBS Lett. 439, 246–252.

[16] Hanck, D.A. and Sheets, M.F. (1995) J. Gen. Physiol. 106, 601-616.

[17] Strichartz, G.R. and Wang, G.K. (1986) J. Gen. Physiol. 88, 413-435.

[18] Little, M.J., Zappia, C., Gilles, N., Connor, M., Tyler, M.I., Martin-Eauclaire, M.-F., Gordon, D. and Nicholson, G.M. (1998) J. Biol. Chem. 273, 27076-27083.

[19] Gilles, N., Leipold, E., Chen, H., Heinemann, S.H. and Gordon, D. (2001) Biochemistry 40, 14576-84.

[20] Gordon, D. (1997) in: Toxins and Signal Transduction, Vol. Cellular And Molecular Mechanisms of Toxin Action Series, pp. 119-149 (Lazarowici, P. and Gutman, Y., Eds.) Harwood Press, Amsterdam.

[21] Laemmli, U.K. (1970) Nature 227, 680-685.

[22] Ginsborg, B.L. and Warriner, J. (1960) Br. J. Pharmacol. 15, 410-411.

[23] Tzeng, M.C. and Tian, S.S. (1983) Toxicon 21, 879-81.

[24] Hamill, O.P., Marty, A., Neher, E., Sakmann, B. and Sigworth, F.J. (1981) Pflügers Archiv. (Eur. J. Physiol.) 391, 85–100.

[25] Ogata, N., Nishimura, M. and Narahashi, T. (1989) J. Pharmacol. Exp. Ther. 248, 605–613.

[26] Roy, M.L. and Narahashi, T. (1992) J. Neurosci. 12, 2104–2111.

[27] Bezanilla, F. and Armstrong, C.M. (1977) J. Gen. Physiol. 70, 594–566.

[28] Eitan, M., Fowler, E., Herrmann, R., Duval, A., Pelhate, M. and Zlotkin, E. (1990) Biochemistry 29, 5941–5947.

[29] Graudins, A., Wilson, D., Alewood, P.F., Broady, K.W. and Nicholson, G.M. (2002) Toxicon 40, 259-266.

[30] Corzo, G., Gilles, N., Satake, H., Villegas, E., Dai, L., Nakajima, T. and Haupt, J. (2003) FEBS Lett 547, 43-50.

[31] Norton, R.S. and Pallaghy, P.K. (1998) Toxicon 36, 1573–1583.

[32] Gilles, N., Harrison, G., Karbat, I., Gurevitz, M., Nicholson, G.M. and Gordon, D. (2002) Eur. J. Biochem. 269, 1500-1510.

[33] Tugarinov, V., Kustanovich, I., Zilberberg, N., Gurevitz, M. and Anglister, J. (1997) Biochemistry 36, 2414–2424.

Figure Legends

Fig. 1. (A-B) SDS-PAGE gel and Western blot of *M. bradleyi* venom. (A) Silver-stained SDS-PAGE gel showing protein components of male and female *M. bradleyi* venom. Left-hand lanes shows high (High MW) and low (Low MW) molecular weight markers. Note a band consistent with δ-MSTX-Mb1a at 4933 Da in whole male venom that is absent in whole female venom. (B) Western blot analysis of male and female *M. bradleyi* venom using Sydney funnel-web spider antivenom. The left-hand lane (MW) contains molecular weight markers. Note a positive reaction consistent with δ-MSTX-Mb1a in whole male venom that is absent in whole female venom. (C-D) Reverse-phase HPLC chromatogram of pooled male *M. bradleyi* venom. (C) Screening of venom fractions revealed that peak *a* caused spontaneous contractions of chick isolated biventer cervicis nerve-muscle preparations. (D) Further rp-HPLC purification of this fraction yielded three major peaks, the largest of which (peak *b*) was found to be the most active component in the chick isolated biventer cervicis nerve-muscle preparation.

Fig. 2. Comparison of the amino acid sequences of δ-MSTX-Mb1a with currently known members of the δ-ACTX family and Magi 4. Identical residues are shaded black and conservatively substituted residues, relative to δ-MSTX-Mb1a, are shaded grey. Toxins are ordered by homology to δ-MSTX-Mb1a. Gaps (dashes) have been inserted to maximise alignment. The disulphide bonding pattern for the strictly conserved cysteine residues determined for δ-ACTX-Ar1a [9] and δ-ACTx-Hv1a [8] is indicated below the sequences; it is assumed that δ-MSTX-Mb1a, δ-ACTX-Hs20.1a [4], δ-ACTX-Hv1b [7] and Magi 4 [30] have the same disulphide bonding pattern. Suspected key residues critical for function [4] are indicated by the

arrows. Secondary structure for δ-ACTX-Hv1a is shown at the top of the figure where shaded rectangles represent β-turns (the type of turn is indicated in the rectangle), black arrows represent β-strands, and the black cylinder represents a 3_{10} α-helix [8]. The percentage identity and homology with δ-MSTX-Mb1a is also shown to the right of the sequences.

Fig. 3. Typical effects of antagonists on responses to δ-MSTX-Mb1a in the isolated chick biventer cervicis nerve-muscle preparation. (A) Development of muscle fasciculation and contracture following addition of 85 nM δ-MSTX-Mb1a. The dotted line indicates the resting tension of the muscle**.** (B-C) Following exposure to 10 μM (+)-tubocurarine (B) or 200 nM TTX (C) 85 nM δ-MSTX-Mb1a fails to alter twitch or resting muscle tension.

Fig. 4. Typical traces showing neutralisation of the effects of δ-MSTX-Mb1a by Sydney funnel-web spider antivenom on the indirectly stimulated chick biventer cervicis nerve-muscle preparation. (A) Funnel-web spider antivenom (FWS-AV, 0.6 Units/ml) was applied to the preparation 10 minutes *prior* to the application of δ-MSTX-Mb1a (85 nM). Note lack of toxin response. (B) FWS-AV (0.6 Units/ml) was applied *following* the application of δ-MSTX-Mb1a (85 nM). Note the rapid return of muscle tension to control levels and reversal of muscle fasciculation.

Fig. 5. Typical effects of δ-MSTX-Mb1a on TTX-sensitive and TTX-resistant I_{Na} in rat dorsal root ganglion neurons. Panels show the effect of δ-MSTX-Mb1a on TTX-sensitive (left-hand) and TTX-resistant (right-hand) I_{Na}. (A and E) Superimposed current traces recorded following a 50 ms depolarisation to -10 mV from a holding potential of –90 mV, before, and 10 min after,

toxin application. (A) Note the reduction in peak current amplitude of TTX-sensitive I_{Na} and slowed inactivation kinetics. (E) Lack of effect of 300 nM δ-MSTX-Mb1a on TTX-resistant I_{Na} elicited by the same stimulus protocol. Both current responses were recorded in the presence of 200 nM TTX to eliminate residual TTX-sensitive I_{Na} . Remaining panels show typical effects of δ-MSTX-Mb1a on the current voltage (I/V) relationship of TTX-sensitive (B-D) and TTX-resistant (F-H) I_{Na} . Families of I_{Na} were evoked by a series of 50-ms depolarisations from –90 to +70 mV in 10-mV steps applied every 10 s from a holding potential of –90 mV. Families of I_{Na} before (B and F) and after (C and G) application of 30 nM δ-MSTX-Mb1a. For clarity, I_{Na} recorded in 20-mV steps are presented. Note that the inactivation kinetics of both inward and outward currents are slowed and incomplete in panel C only. (D and H) Peak (circles) and late (triangles) I/V relationships are shown before (empty symbols) and following (filled symbols) a 10 min perfusion with 30 nM δ-MSTX-Mb1a. Late currents were measured at the end of each 50 ms depolarising test pulse. Peak and late currents were fitted according to Equation 1 described in the Materials and methods. Note that no shift in the threshold of activation is seen in panel H.

Figure 1

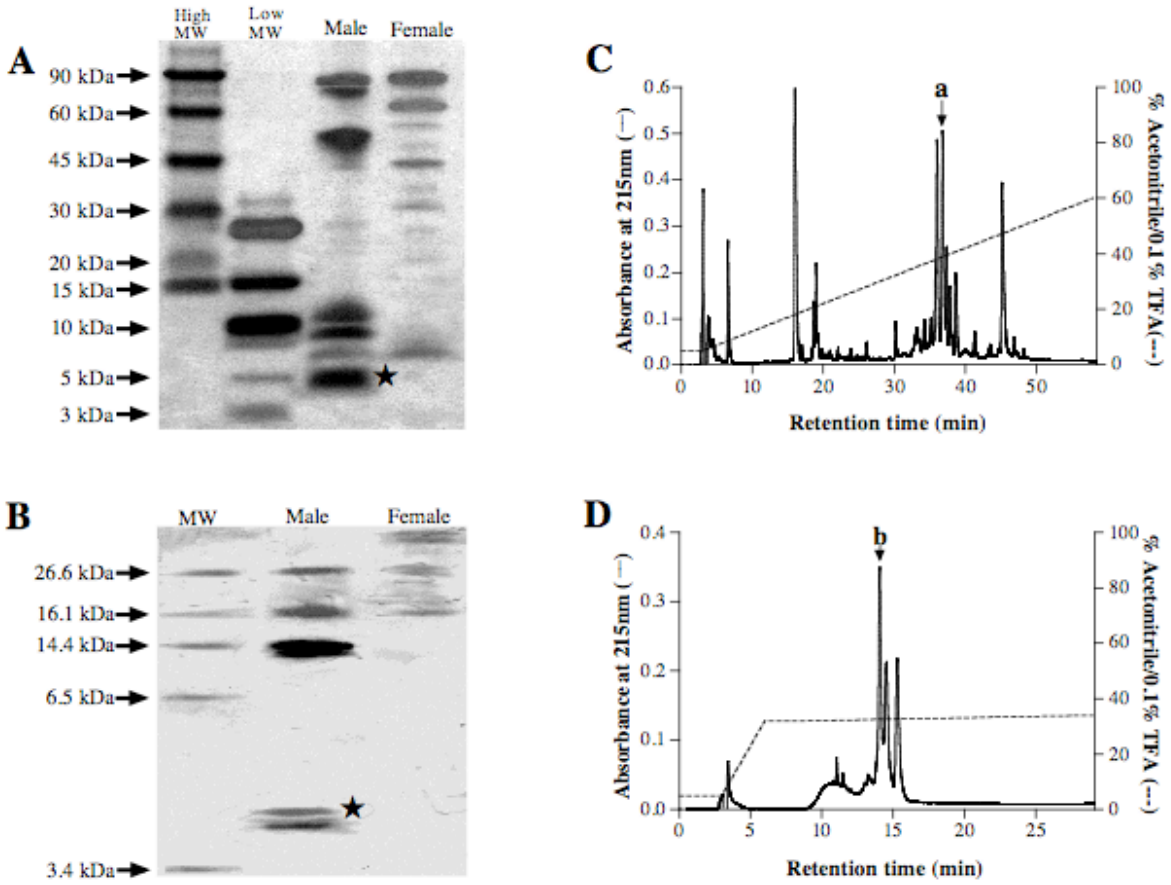
A
High MW
Low MW
Male
Female
90 kDa
60 kDa
45 kDa
30 kDa
20 kDa
15 kDa
10 kDa
5 kDa
3 kDa
B
MW
Male
Female
26.6 kDa
16.1 kDa
14.4 kDa
6.5 kDa
3.4 kDa
C
a
Absorbance at 215nm (—)
% Acetonitrile/0.1 % TFA(---)
Retention time (min)
D
b
Absorbance at 215nm (—)
% Acetonitrile/0.1% TFA (---)
Retention time (min)

Figure 2

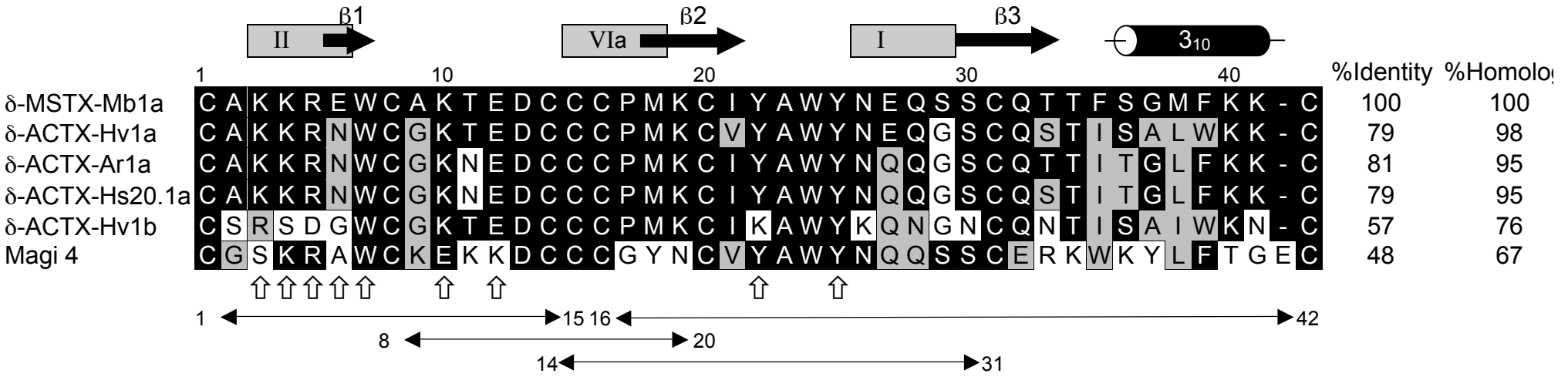
β1
β2
β3
II
VIa
I
3_{10}
1
10
20
30
40
%Identity
%Homolog
δ-MSTX-Mb1a C A K K R E W C A K T E D C C C P M K C I Y A W Y N E Q S S C Q T T F S G M F K K - C 100 100
δ-ACTX-Hv1a C A K K R N W C G K T E D C C C P M K C V Y A W Y N E Q G S C Q S T I S A L W K K - C 79 98
δ-ACTX-Ar1a C A K K R N W C G K N E D C C C P M K C I Y A W Y N Q Q G S C Q T T I T G L F K K - C 81 95
δ-ACTX-Hs20.1a C A K K R N W C G K N E D C C C P M K C I Y A W Y N Q Q G S C Q S T I T G L F K K - C 79 95
δ-ACTX-Hv1b C S R S D G W C G K T E D C C C P M K C I K A W Y K Q N G N C Q N T I S A I W K N - C 57 76
Magi 4 C G S K R A W C K E K K D C C C G Y N C V Y A W Y N Q Q S S C E R K W K Y L F T G E C 48 67
1
15 16
42
8
20
14
31

.

Figure 3

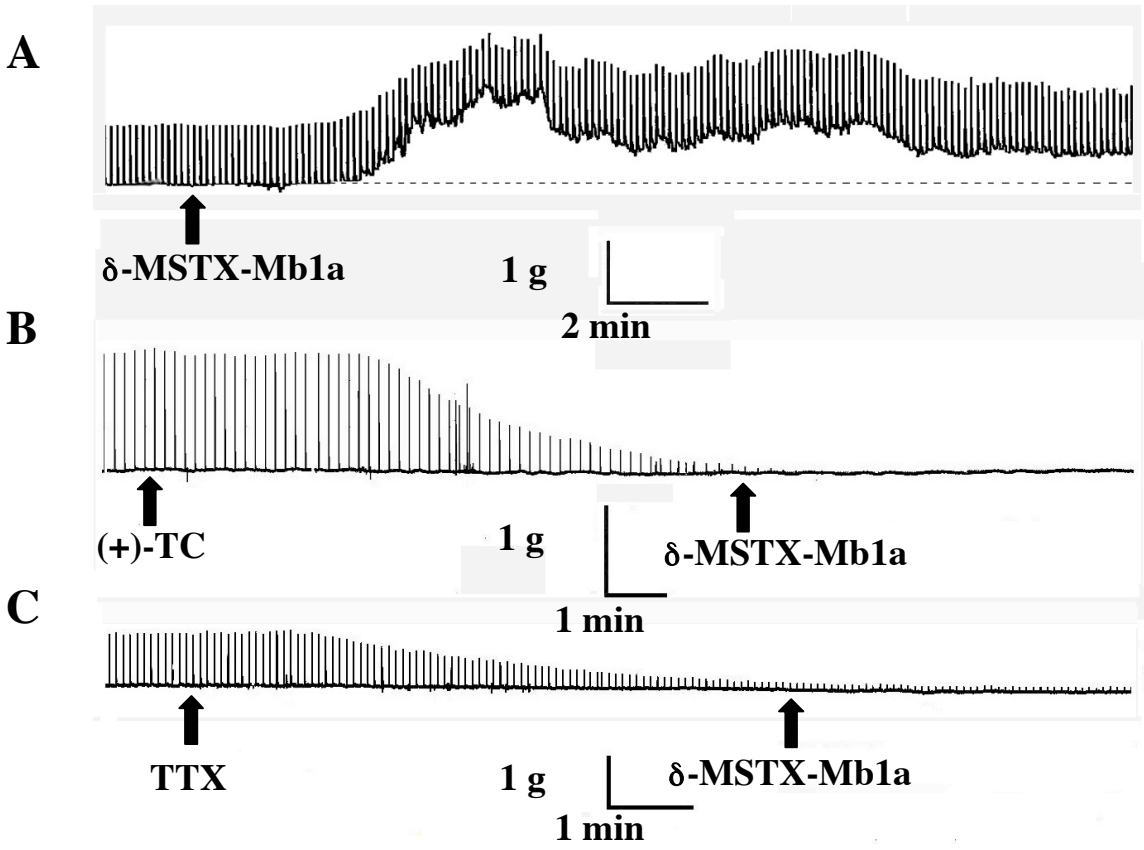
A
δ-MSTX-Mb1a
1 g
2 min
B
(+)-TC
1 g
δ-MSTX-Mb1a
1 min
C
TTX
1 g
δ-MSTX-Mb1a
1 min

Figure 4

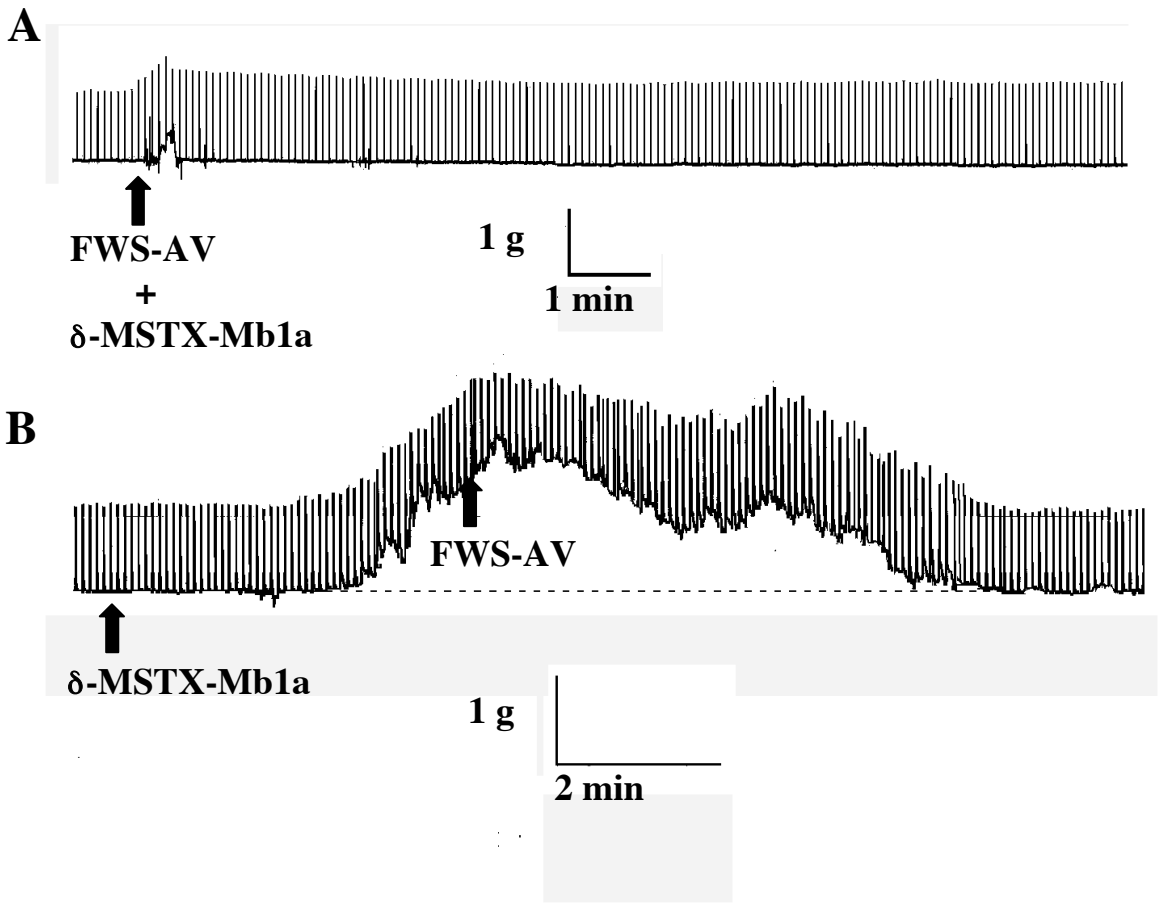

Figure 5

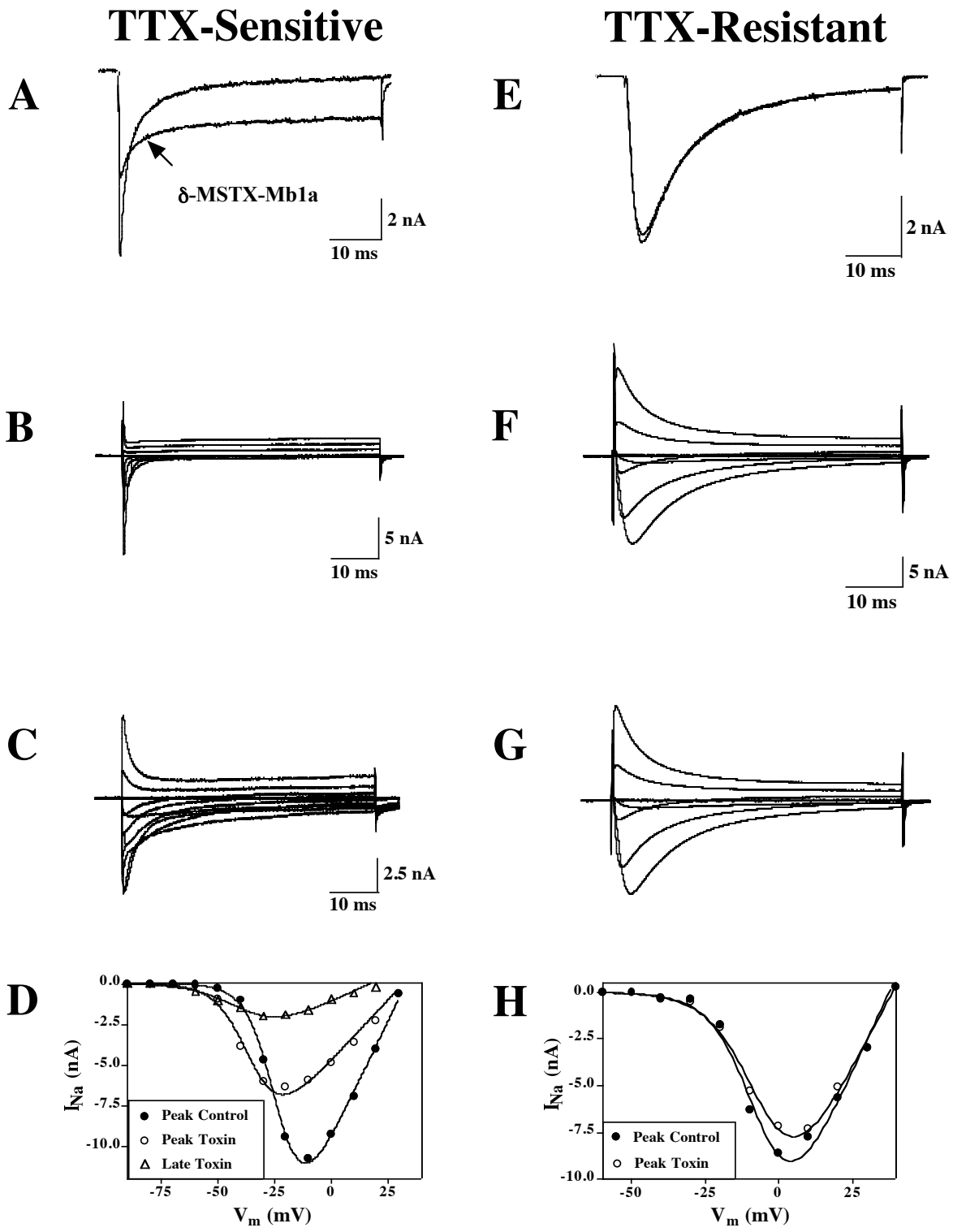
TTX-Sensitive
TTX-Resistant
A
δ-MSTX-Mb1a
2 nA
10 ms
E
2 nA
10 ms
B
5 nA
10 ms
F
5 nA
10 ms
C
2.5 nA
10 ms
G
D
H
I_{Na} (nA)
Peak Control
Peak Toxin
Late Toxin
V_m (mV)
Peak Control
Peak Toxin
V_m (mV)

Figure 3

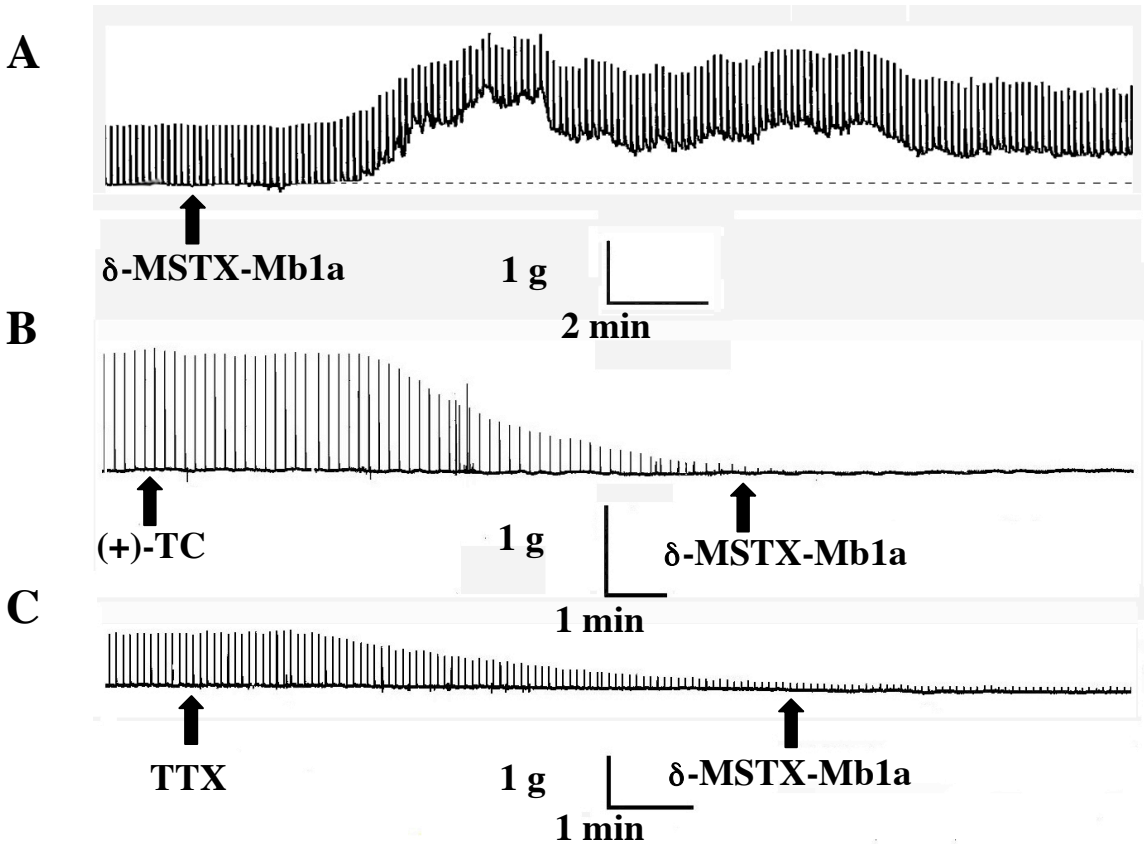
A
δ-MSTX-Mb1a
1 g
2 min
B
(+)-TC
1 g
δ-MSTX-Mb1a
1 min
C
TTX
1 g
δ-MSTX-Mb1a
1 min

Figure 4

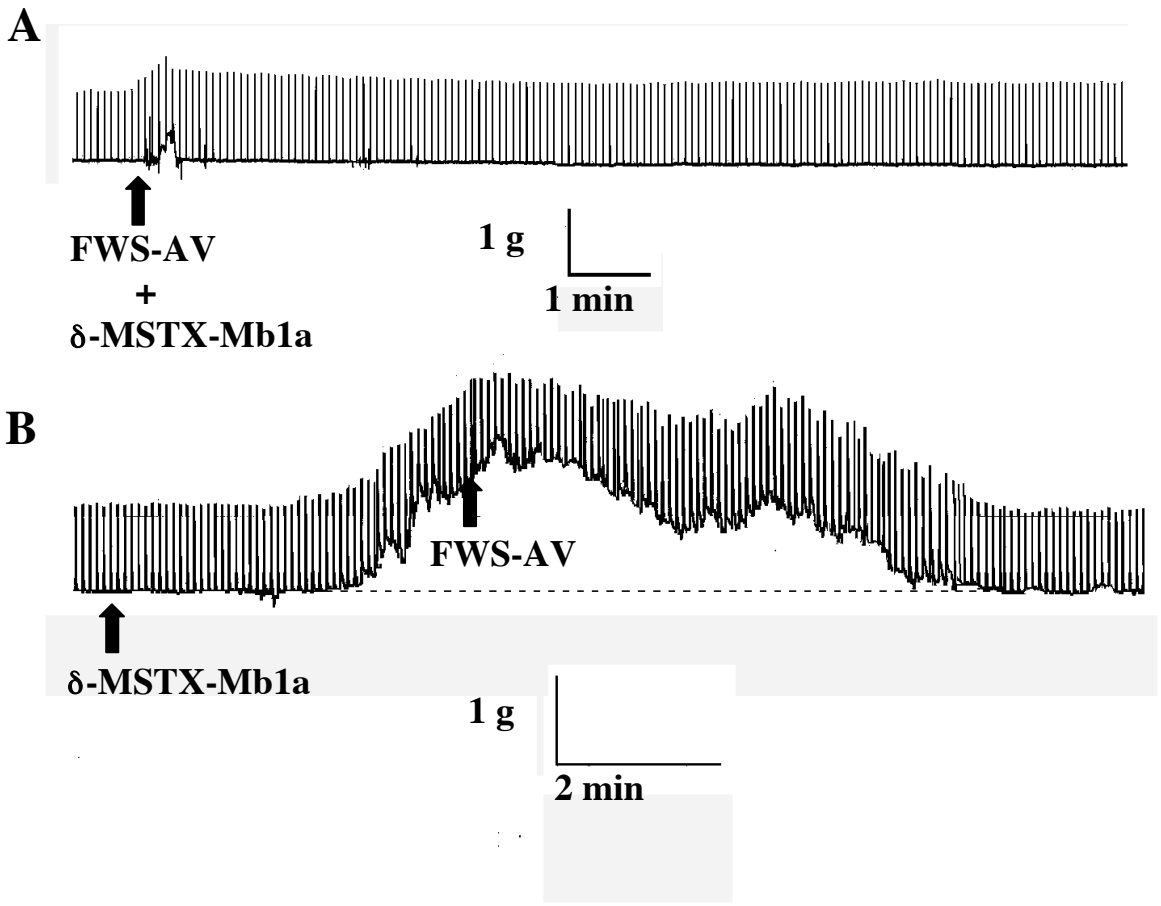

Figure 5

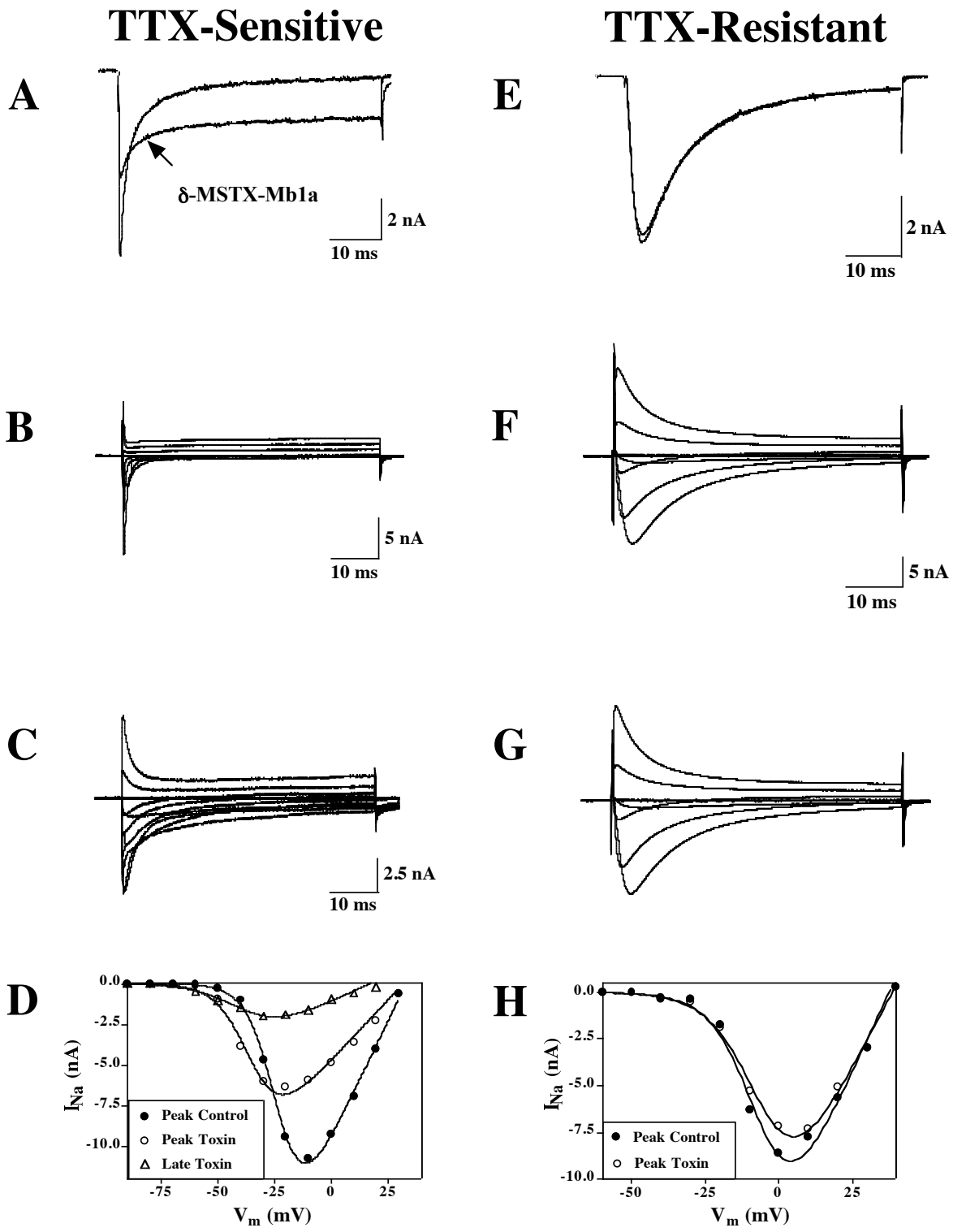
TTX-Sensitive
TTX-Resistant
A
δ-MSTX-Mb1a
2 nA
10 ms
E
2 nA
10 ms
B
5 nA
10 ms
F
5 nA
10 ms
C
2.5 nA
10 ms
G
D
H
I_{Na} (nA)
Peak Control
Peak Toxin
Late Toxin
V_m (mV)
Peak Control
Peak Toxin
V_m (mV)